

Local moments near the metal-insulator transition

Subir Sachdev

Center for Theoretical Physics, Yale University, P.O. Box 6666, New Haven, Connecticut 06511

(Received 27 June 1988)

This paper examines in detail the phenomenological local-moment model Hamiltonian used recently by Paalanen, Graebner, Bhatt, and Sachdev [Phys. Rev. Lett. **61**, 597 (1988)] to understand experiments on metallic phosphorus-doped silicon near the metal-insulator transition. The model describes the disordered metal in terms of two components: itinerant quasiparticles which lead to charge transport and electron local moments. Fermi-liquid properties of the itinerant quasiparticles in the presence of the low-energy spin fluctuations of the local moments are calculated. The local moments lead to strong spin-flip quasielastic scattering of the itinerant electrons; this scattering leads to a temperature dependence of the conductivity and modifies quantum-interference effects near the metal-insulator transition.

I. INTRODUCTION

The metal-to-insulator transition (MIT) in doped semiconductors has been the subject of a large number of careful experiments and theoretical analyses in the past decade.¹⁻⁵ Most of the theoretical work has concentrated on examining the effects of disorder on the metallic state by a weak-disorder perturbation theory. Supplemented by renormalization-group methods such a perturbation theory can yield information about the metal all the way up to the MIT. Building upon earlier work of Finkelstein and Castellani *et al.*,³ Castellani, Kotliar, and Lee⁴ have recently succinctly stated the predictions of such a perturbative renormalization-group approach. A central result of this approach has been the prediction of an enhancement in the triplet Fermi-liquid interaction parameter (A_0^g), as the strength of the disorder is increased or the temperature is lowered, in a system with spin-independent impurity scattering. The increase in A_0^g then leads to an enhancement of the static spin susceptibility of the metal; right at the MIT the spin susceptibility is predicted to diverge at zero temperature.

In a recent experiment, Paalanen *et al.*^{1,5,6} performed a detailed comparison of the theoretical predictions with the temperature dependence of transport (conductivity) and thermodynamic (spin-susceptibility and specific-heat) properties of metallic phosphorus-doped silicon (Si:P) close to the MIT. They found that the scaling theories of Finkelstein³ and Castellani *et al.*⁴ significantly underestimated the enhancement of the spin susceptibility. Instead, a simple phenomenological two-fluid model was found to reproduce the temperature dependences of the spin susceptibility and specific heat very accurately. In this model the metallic state was assumed to be made up of two distinct components: (i) a fluid of itinerant quasiparticles, which contributes a finite conductivity, and (ii) electron local moments, which are distributed randomly throughout the system; no charge transport is allowed between the local moment and the rest of the system, but its spin is coupled via exchange interactions with the other electrons. The local moments have a large, almost

Curie-like, spin susceptibility and can therefore account for the experimentally observed enhancement of the spin susceptibility. Similar models of the metallic state have been discussed earlier in Refs. 7 and 8 and were also used by Alloul and Dellouve⁹ to understand their nuclear magnetic resonance experiments on Si:P.

There is at present no complete first-principles theory which can explain the success of the phenomenological two-fluid model in describing the experiments on Si:P. The enhancement of A_0^g in the perturbative theories³ can perhaps be interpreted as signaling an instability of a disordered Fermi liquid towards the trapping of some electrons in local-moment states. The determination of the precise mechanism of this instability is clearly an important outstanding problem whose solution will need a deeper understanding of the effects of Coulomb interactions in the presence of disorder; this is an issue which shall *not* be addressed in this paper. Instead, we shall take the success in explaining the experiments^{1,9} as sufficient reason to conclude that the phenomenological two-fluid Hamiltonian contains all of the important low-energy excitations of a metallic system of interacting electrons in the presence of strong disorder.

The main purpose of this paper is to develop a complete theory of the properties of the phenomenological two-fluid Hamiltonian. All previous analyses of this Hamiltonian have been very simple-minded; the itinerant electrons were treated as noninteracting fermions, and all interactions between the local moments and the itinerant electrons were ignored. One of the important consequences of developing a precise theory will be the discovery of a new source-temperature dependence for the conductivity.

It is useful at this point to state more precisely the structure of the model Hamiltonian H . It consists of four parts: $H = H_C + H_{\text{dis}} + H_{LM} + H_{\text{int}}$. We describe each component briefly here, with the details being spelled out in Sec. II.

(i) $H_C + H_{\text{dis}}$ describes the disordered Fermi liquid formed by itinerant electrons moving in a random potential. Betbeder-Matibet and Nozières^{10,11} have presented a

complete analysis of the Fermi-liquid properties of this model.

(ii) $H_{LM} = \sum_{ij} J_{ij} \mathbf{S}(\mathbf{R}_i) \cdot \mathbf{S}(\mathbf{R}_j)$ describes the spin- $\frac{1}{2}$ local moments \mathbf{S} at the spatial positions \mathbf{R}_i with mutual antiferromagnetic exchange interactions J_{ij} . On the insulating side of the transition, H_{LM} is the complete Hamiltonian. In the insulator, J_{ij} falls off exponentially with $|\mathbf{R}_i - \mathbf{R}_j|$, which leads to a broad distribution in the values of $\log(J_{ij})$ at different sites.¹² We shall assume that this broad distribution persists on the metallic side. This will lead to large variations in $\omega_{\mathbf{R}}$, the frequency at which the spectral weight of the local-moment spin fluctuations at the site \mathbf{R} is peaked.

(iii) $H_{\text{int}} = \sum_{\mathbf{R}} K_{\mathbf{R}} \mathbf{S}(\mathbf{R}) \cdot \mathbf{s}(\mathbf{R})$ describes the interaction between the local moments and the conduction electrons, where \mathbf{s} is the spin of the itinerant electrons, and the $K_{\mathbf{R}}$ are exchange constants. We shall assume throughout that the temperature is large enough so that all Kondo-like effects can be neglected (this condition appears to be satisfied by all current experiments⁶). Paalanen *et al.*¹ implicitly considered a Hamiltonian consisting of H_C , H_{dis} , and H_{LM} . The interaction H_{int} has not been considered before.

Before describing the physical properties of H , it will be necessary to make a few statements about our methodology and the structure of the itinerant-electron Green's functions. We find that the interaction between the itinerant electrons and the local moments leads to a strong frequency dependence in the self-energy of the itinerant electrons. This frequency dependence can be dealt with by techniques used previously in the context of the electron-phonon interactions¹³ and the heavy-fermion problem.¹⁴ The interactions in H_C and H_{int} lead to the following structure in the itinerant-quasiparticle retarded Green's function G^R for small frequencies ω and momenta \mathbf{k} near the Fermi surface:

$$G^R(\mathbf{k}, \omega) = \frac{a_C}{\omega Z - (k_F/m_C)(k - k_F) + i(1/2\tau_e + 1/2\tau_{qe}^s)}, \quad (1.1)$$

where k_F is the Fermi wave vector, m_C is the effective mass, and a_C the quasiparticle residue, arising from just the Coulomb interactions, and τ_e the elastic scattering time arising from H_{dis} . The spin-flip quasielastic scattering time τ_{qe}^s and the frequency renormalization factor Z are *temperature dependent* and arise from the interaction of the itinerant electrons with the local moments (H_{int}) and are given by

$$Z(T) \approx 1 + \frac{3N_C a_C^2}{2} \sum_{\mathbf{R} \in \mathcal{L}_d} K^2(\mathbf{R}) \int_0^\infty d\Omega \frac{D(\Omega, \mathbf{R})}{\Omega} \quad (1.2)$$

and

$$\frac{1}{\tau_{qe}^s}(T) \approx \frac{3\pi N_C a_C^2}{2} \sum_{\mathbf{R} \in \mathcal{L}_s} K^2(\mathbf{R}) \times \int_0^\infty d\Omega D(\Omega, \mathbf{R}) \coth \left[\frac{\Omega}{2T} \right], \quad (1.3)$$

where $N_C = m_C k_F / (2\pi^2)$ is the itinerant quasiparticle density of states and $D(\Omega, \mathbf{R})$ is the spectral weight of the local-moment spin fluctuations at the site \mathbf{R} ; as noted earlier, $D(\Omega, \mathbf{R})$ is peaked at a frequency $\omega_{\mathbf{R}}$ which fluctuates over several orders of magnitude from site to site. The sum over \mathbf{R} in the two expressions extends over two disjoint sets of local-moment sites \mathcal{L}_s and \mathcal{L}_d . The set of local-moment sites \mathcal{L}_s contributing to τ_{qe}^s satisfies $\omega_{\mathbf{R}} < T$, while the set \mathcal{L}_d contributing to Z are the remaining local moments. The temperature dependence of Z arises from the temperature-dependent condition $\omega_{\mathbf{R}} > T$, which determines the sites belonging to \mathcal{L}_d . The quasistatic nature of the spin fluctuations on the local-moment sites in \mathcal{L}_s is the reason for describing the scattering time τ_{qe}^s as quasielastic. The results (1.1)–(1.3) have been obtained from the expressions (2.11)–(2.13) after analytic continuation to real frequencies. The density-polarization function Π^d and the spin-response function χ^s of the itinerant quasiparticles are also calculated in the hydrodynamic limit and have the following form:

$$\begin{aligned} \Pi^d(q, \omega) &= N_C \frac{Dq^2}{Dq^2(1 + F_{0C}^s) - i\omega} \\ \chi^s(q, \omega) &= N_C \frac{Dq^2 + 4/(3\tau_{qe}^s) - i\omega(4Z - 4)/3}{[Dq^2 + 4/(3\tau_{qe}^s) - i\omega(4Z - 4)/3](1 + \bar{F}^a) - i\omega}, \end{aligned} \quad (1.4)$$

where the diffusion constant D is given by

$$D = \frac{k_F^2 \tau}{(3m_C^2)}, \quad \frac{1}{\tau} = \frac{1}{\tau_e} + \frac{1}{\tau_{qe}^s}, \quad (1.5)$$

F_{0C}^s is a Fermi-liquid constant arising from H_C , and \bar{F}^a is a Fermi-liquid constant involving both the Coulomb interactions (H_C) and the local-moment interactions (H_{int}); an explicit expression for \bar{F}^a is given in Eq. (2.6). The thermodynamic response functions above follow from the analytic continuation of Eq. (2.31) to real frequencies. The important point to note here is that F_{0C}^s and \bar{F}^a are both *temperature independent*.

We are now finally in a position to state the consequences of our analysis of H upon the physics of the system. Using the response functions above, we find the following.

(i) The compressibility of the itinerant electrons is $N_C / (1 + F_{0C}^s)$ and is unaffected by the presence of the local moments. In particular the frequency renormalization factor Z (which can also be interpreted as a dynamic effective-mass renormalization) has no effect. The same phenomenon occurs in the phenomenological theories of heavy fermions.¹⁴

(ii) The static spin susceptibility of the itinerant electrons is $N_C / (1 + \bar{F}^a)$. As the presence of the local moments leads to a *decrease* in the value of \bar{F}^a , there is an enhancement in the value of the spin susceptibility. However, there is no simple relationship between the value of the temperature-dependent quantity Z and the temperature-independent enhancement of the spin susceptibility. This feature is also applicable to the phenom-

enological model of heavy fermions used by Miyake *et al.*¹⁵

(iii) The above two results justify the neglect of H_{int} in the comparison with experiment of the *thermodynamic properties* performed in Ref. 1. The presence of H_{int} simply leads to a temperature-independent renormalization of the itinerant-electron contribution.

(iv) It is not correct, however, to neglect H_{int} for the *transport properties*. The conductivity of the system can be determined from the Einstein relation $\sigma = e^2 N_C D$ and the expression for D above [Eq. (1.5)]. The presence of the local moments therefore leads to a temperature-dependent decrease in the conductivity via the temperature dependence of τ_{qe}^s . This prediction is compared with experiments on Si:P in Sec. IV. Note also that the frequency renormalization scale Z is absent from the conductivity.

(v) We have so far ignored the perturbative quantum-interference effects, which are an important ingredient of the scaling theories.^{3,4} These are, in principle, present in H through the interactions in $H_C + H_{\text{dis}}$. However, the interaction of the itinerant electrons with the local moments (H_{int}) modifies the magnitude of these corrections. Because the energy transferred in the quasielastic scattering events is much smaller than kT , $(\tau_{qe}^s)^{-1}$ acts as a cutoff for long-wavelength fluctuations in the singlet and triplet particle-particle, and the triplet particle-hole ladders of the itinerant quasiparticles. The interactions in H_{int} therefore *suppress the perturbative quantum interference effects of the scaling theories*. It is therefore *not* correct to describe the MIT by using the perturbative renormalization-group theory^{3,4} on the itinerant quasiparticles while assuming that the electron local moments are an independent component of the system whose sole physical effect is to enhance the spin susceptibility. This effect of the spin-flip quasielastic scattering may also be important in understanding the difference in the transport properties between compensated and uncompensated semiconductors.⁶

It is clear from the above discussion that τ_{qe}^s is an important quantity characterizing the effect of the local moments. Using Eq. (1.3) we will show that

$$\frac{1}{\tau_{qe}^s} \propto T \chi^L(T), \quad (1.6)$$

where χ^L is the *local-moment* contribution to the spin susceptibility. This relationship predicts the $1/\tau_{qe}^s$ falls off as $T^{1-\alpha}$ with falling temperatures. The exponent $\alpha > 0$ characterizes the divergence of the spin susceptibility.¹² At low enough temperatures, therefore, $1/\tau_{qe}^s$ should become larger than kT . An experimental test of the temperature dependence of the conductivity implied by Eq. (1.6) is carried out in Sec. IV.

A separate but related issue addressed in this paper is whether the spin relaxation time τ_{qe}^s will appear as a linewidth in the electron-spin-resonance (ESR) spectrum. A naive extension of Eq. (1.4) to finite magnetic fields would predict that $4/(3\tau_{qe}^s)$ contributes to the linewidth of the itinerant-electron portion of the ESR spectrum. However, as the g factors of the itinerant electrons and

the local moments are equal, the interaction between the local moments and the itinerant electrons conserves total spin and leads to no loss of spin coherence. On the basis of very general arguments we therefore expect the ESR spectrum of H to be a δ function (this is the well-known bottleneck effect¹⁶). These principles are illustrated in a simple Anderson model¹⁷ calculation in Sec. III. Unlike the model considered in Sec. II, the simplicity of this model allows calculation of the all mutual correlation functions between the local moments and the itinerant electrons. The results of this calculation (i) confirm the validity of Eq. (1.4) for the itinerant-electron spin correlation function, and (ii) show that at low frequencies and magnetic fields, $\omega, h \ll T$, the *total* spin susceptibility χ_t (involving the sum of itinerant-electron and local-moment contributions and their cross correlations) satisfies

$$\chi_t(\mathbf{q}=\mathbf{0}, \omega) = \chi_t(\mathbf{q}=\mathbf{0}, \omega=0) \frac{h}{h-\omega}, \quad (1.7)$$

which predicts a δ -function ESR spectrum. In ESR experiments on Si:P,¹⁸ the dominant contribution to the linewidth at low temperatures comes from the relaxation of the local moments by their hyperfine interaction A with the phosphorus nuclear spins;¹⁹ the rapid exchange of magnetization between the local moments and itinerant electrons motionally narrows the linewidth from $A/2$ to approximately $A/25$.⁹

The outline of the rest of the paper is follows. In Sec. II we consider the general Fermi-liquid properties of a system of itinerant electron interacting with a dilute concentration of local moments. Section III illustrates the principles of Sec. II by an explicit calculation on a disordered Anderson model. We also calculate the total electronic-spin susceptibility in this section and show that it obeys Eq. (1.7). Application of the theories of this paper to various experiments is discussed in Sec. IV. Finally, Sec. V reiterates the main conclusions of this paper.

II. FERMI-LIQUID THEORY

This section presents details of the Fermi-liquid properties of itinerant electrons moving in a random potential with mutual Coulomb interactions and exchange interactions with a dilute concentration of local moments.

The Coulomb interactions of the itinerant electrons are described by H_C :

$$H_C = \sum_{\mathbf{k}, \alpha} \frac{k^2}{2m} c_{\mathbf{k}, \alpha}^\dagger c_{\mathbf{k}, \alpha} + \frac{1}{2} \sum_{\mathbf{k}_1, \mathbf{k}_2, \mathbf{q}} \sum_{\alpha, \beta} \frac{4\pi e^2}{q^2} c_{\mathbf{k}_1 + \mathbf{q}, \alpha}^\dagger c_{\mathbf{k}_2 - \mathbf{q}, \beta}^\dagger c_{\mathbf{k}_2, \beta} c_{\mathbf{k}_1, \alpha}, \quad (2.1)$$

where $c_{\mathbf{k}, \alpha}$ is the destruction operator for an electron of mass m with momentum \mathbf{k} and spin α . Conventional Fermi-liquid theory¹⁰ tells us that at low temperatures ($T \ll E_F$, the Fermi energy) the single-particle Green's functions of these electrons can be written as the sum of quasiparticle and nonquasiparticle pieces:

$$G_C(\mathbf{k}, \omega_n) = \frac{a_C}{i\omega_n - (k_F/m_C)(k - k_F)} + \phi(\mathbf{k}, \omega_n), \quad (2.2)$$

where ϕ is the incoherent nonquasiparticle piece of the Green's functions which has no singularities near the Fermi surface. We are using the Matsubara finite-temperature formalism and ω_n is the Matsubara frequency. The subscript C has been added to the parameters to emphasize that they depend only upon H_C , the Coulomb part of the Hamiltonian.

The local-moment part of the Hamiltonian H_{LM} is given by

$$H_{LM} = \sum_{i,j} J_{ij} \mathbf{S}(\mathbf{R}_i) \cdot \mathbf{S}(\mathbf{R}_j), \quad (2.3)$$

where $\mathbf{S}(\mathbf{R})$ is the spin- $\frac{1}{2}$ operator of the local moment at the site \mathbf{R} . As noted earlier, the properties of H_{LM} were examined on the insulating side of the metal-insulator transition in Ref. 12. In the insulator, the exchange constants J_{ij} are known to fall off exponentially with the separation between \mathbf{R}_i and \mathbf{R}_j . This exponential dependence of the exchange constants leads to a broad distribution in the values of $\log(J_{ij})$. As a consequence, Bhatt and Lee¹² showed that the ground state of H_{LM} can be understood as a condensation of nearest-neighbor pairs of spins into tightly bound singlets. The condensation energy of these pairs varied over several orders of magnitude because of the variations in the magnitude of J . The large variation in the strength of J_{ij} will be assumed to persist onto the metallic side of the transition. The presence of the itinerant electrons will lead to an additional Ruderman-Kittel-Kasuya-Yosida (RKKY) coupling between the local moments, which could be much larger than the direct-exchange coupling J_{ij} . Our assumptions of the nature of the local-moment spin fluctuations can be stated more precisely in terms of the time-ordered spin-correlation functions

$$\begin{aligned} \mathcal{D}(\Omega_n, \mathbf{R}_i, \mathbf{R}_j) &= \frac{1}{3} \int_0^\beta d\tau \langle T_\tau [\mathbf{S}(\mathbf{R}_i, 0) \cdot \mathbf{S}(\mathbf{R}_j, \tau)] \rangle \\ &= - \int d\omega \frac{D(\omega, \mathbf{R}_i, \mathbf{R}_j)}{i\Omega_n - \omega}, \end{aligned} \quad (2.4)$$

where we have introduced the usual Lehmann spectral weight decomposition of the spin-correlation function. After we average over the positions of the local moments, the only quantity which enters into the Fermi-liquid properties of the itinerant electrons is the diagonal part of the spectral weight $D(\omega, \mathbf{R}, \mathbf{R})$. The only assumptions we shall make about the nature of the local-moment spin fluctuations can now be stated as follows. (i) For a given \mathbf{R} , $D(\omega, \mathbf{R}, \mathbf{R})$ is peaked at frequency $\omega_{\mathbf{R}}$, which is of the order of the exchange constants with which the spin at \mathbf{R} interacts with the other local moments. (ii) The frequency $\omega_{\mathbf{R}}$ varies over several orders of magnitude as a function of the local-moment position \mathbf{R} . As noted in the Introduction, site with $\omega_{\mathbf{R}} < T$ will have a very different effect upon the properties of the itinerant electrons from the sites with $\omega_{\mathbf{R}} > T$.

The interaction between the local moments and the itinerant electrons is described by H_{int} :

$$H_{\text{int}} = \frac{1}{2V} \sum_{\mathbf{R}} \sum_{\mathbf{k}_1, \mathbf{k}_2} \sum_{\alpha, \beta, \mu} K(\mathbf{R}) S^\mu(\mathbf{R}) c_{\mathbf{k}_1, \alpha}^\dagger \sigma_{\alpha\beta}^\mu c_{\mathbf{k}_2, \beta} \times e^{i(\mathbf{k}_1 - \mathbf{k}_2) \cdot \mathbf{R}}, \quad (2.5)$$

where we have introduced the exchange constant $K(\mathbf{R})$, and σ^μ are Pauli spin matrices measuring the spin of the itinerant electrons. The effect of disorder is represented by a distribution of s -wave scattering potentials

$$H_{\text{dis}} = \sum_{\mathbf{R}_{\text{imp}}} \sum_{\alpha} \int d\mathbf{r} v_{\text{imp}}(\mathbf{r} - \mathbf{R}_{\text{imp}}) \psi_\alpha^\dagger(\mathbf{r}) \psi_\alpha(\mathbf{r}), \quad (2.6)$$

where $v_{\text{imp}}(\mathbf{r}) = v\delta(\mathbf{r})$ is the s -wave scattering potential and ψ_α is Fourier transform of $c_{\mathbf{k}, \alpha}$.

The rest of this section examines the effect of H_{int} and H_{LM} upon the Fermi-liquid properties of the itinerant electrons. The discussion is divided into two subsections: the first subsection deals with changes in the single-particle Green's functions, while the second subsection examines the forms of the vertex and response functions.

A. Itinerant-electron self-energy

In this subsection we will calculate the self-energy Σ which modifies the itinerant-electron Green's function as follows:

$$G^{-1} = G_C^{-1} - \Sigma. \quad (2.7)$$

The random impurities contribute the usual elastic scattering term to the self-energy:

$$\begin{aligned} a_C \Sigma(\mathbf{k}_1, \mathbf{k}_2, \omega_n) &= -i \text{sgn}(\omega_n) \pi N_C a_C^2 v^2 \delta_{\mathbf{k}_1, \mathbf{k}_2} \\ &\equiv -i \text{sgn}(\omega_n) \frac{1}{2\tau_e} \delta_{\mathbf{k}_1, \mathbf{k}_2}. \end{aligned} \quad (2.8)$$

The lowest nontrivial contribution of the local moments to the itinerant-electron self-energy is represented by the Feynman diagram in Fig. 1(a). Analytically this can be represented as follows:

$$\begin{aligned} a_C \Sigma(\mathbf{k}_1, \mathbf{k}_2) &= \frac{3}{4} \sum_{\mathbf{R}_1, \mathbf{R}_2} \sum_{\mathbf{p}} T \sum_{\epsilon_n} K^2(\mathbf{R}) \mathcal{D}(\omega_n - \epsilon_n, \mathbf{R}_1, \mathbf{R}_2) G(\mathbf{p}, \epsilon_n) \\ &\quad \times e^{i(\mathbf{k}_1 - \mathbf{p}) \cdot \mathbf{R}_1 - i(\mathbf{k}_2 - \mathbf{p}) \cdot \mathbf{R}_2}. \end{aligned} \quad (2.9)$$

We will in the subsequent discussion neglect all components of the self-energy which are off-diagonal in momentum space. We expect these off-diagonal components to phase average to zero if the positions of the local moments are uncorrelated with each other. All self-energies and Green's functions will henceforth carry only one momentum index, implicitly referring to their diagonal components. We will also label the local-moment spin-correlation function and spectral weight by one spatial index \mathbf{R} . The momentum integration over the diagonal component of Eq. (2.9) can be easily evaluated if we make the assumption that the itinerant-electron Fermi energy E_F is much larger than any of the frequencies $\omega_{\mathbf{R}}$; this assumption is similar to that made in the electron-phonon problem²⁰ and is easily satisfied in the present sit-

uation. The result is *independent* of the momentum \mathbf{k} and the diagonal portion of the itinerant-electron self-energy $\Sigma(\mathbf{k}, \mathbf{k}, \omega_n) \equiv \Sigma(\omega_n)$ has the following simple form:

$$\Sigma(\omega_n) = -i \frac{\pi N_C a_C}{4} \sum_{\mathbf{R}} T \sum_{\epsilon_n} K^2(\mathbf{R}) \mathcal{D}(\omega_n - \epsilon_n, \mathbf{R}) \text{sgn}(\epsilon_n). \quad (2.10)$$

The large variation in the magnitude of $\omega_{\mathbf{R}}$ distinguishes two different types of contributions to Σ . Let us represent the set of local-moment positions by the symbol \mathcal{L} . The evaluation of the frequency summation in Eq. (2.10) divides \mathcal{L} into the two sets \mathcal{L}_s and \mathcal{L}_d : the sites in \mathcal{L}_s satisfy $\omega_{\mathbf{R}} < |\omega_n|$ (the local-moment spin fluctuations on these sites are *quasistatic*); while the sites in \mathcal{L}_d satisfy $\omega_{\mathbf{R}} > |\omega_n|$ and the *dynamic* nature of the local-moment fluctuations on these sites is important.

Let us first examine the contributions of the sites in \mathcal{L}_s . Since $\mathcal{D}(\Omega_n, \mathbf{R})$ is roughly a Lorentzian peaked at $\Omega_n = 0$ with a width of order $\omega_{\mathbf{R}}$, the sgn function in Eq. (2.10) can be taken out of the summation to yield the following contribution to Σ :

$$\begin{aligned} a_C \Sigma(\omega_n) &\approx -i \frac{3\pi N_C a_C^2}{4} \text{sgn}(\omega_n) \\ &\times \sum_{\mathbf{R} \in \mathcal{L}_s} T \sum_{\Omega_n} K^2(\mathbf{R}) \mathcal{D}(\Omega_n, \mathbf{R}) \\ &\equiv -\text{sgn}(\omega_n) \frac{i}{2\tau_{qe}^s}. \end{aligned} \quad (2.11)$$

$$\begin{aligned} a_C \Sigma(\omega_n) &\approx -i \frac{3N_C \pi a_C^2}{4} \sum_{\mathbf{R} \in \mathcal{L}_d} K^2(\mathbf{R}) \mathcal{D}(\Omega_n = 0, \mathbf{R}) T \sum_{\epsilon_n < |\omega_n|} 1 \\ &= -i\omega_n \frac{3N_C a_C^2}{4} \sum_{\mathbf{R} \in \mathcal{L}_d} K^2(\mathbf{R}) \mathcal{D}(\Omega_n = 0, \mathbf{R}) \equiv i\omega_n (1 - Z). \end{aligned} \quad (2.12)$$

Combining the contributions of Eqs. (2.8), (2.11), and (2.12) to the itinerant-electron self-energy, we obtain finally the following expression for the quasiparticle portion of the itinerant-electron Green's function:

$$G(\mathbf{k}, \omega_n) = \frac{a_C}{i\omega_n Z - (k_F/m_C)(k - k_F) + i \text{sgn}(\omega_n)(1/2\tau_e + 1/2\tau_{qe}^s)}, \quad (2.13)$$

where the values of τ_e , τ_{qe}^s , and Z are given in Eqs. (2.8), (2.11), and (2.12), respectively. Analytically continuing onto the real frequency axis leads to the expressions in Eq. (1.1) for the retarded Green's function.

B. Response functions

The density- and spin-correlation functions of the itinerant electrons will now be evaluated in a conserving approximation consistent with the expressions for Σ . The momentum independence of Σ (which followed from

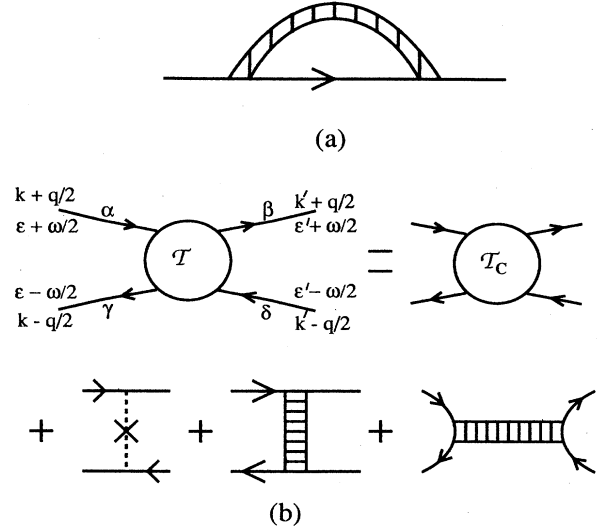


FIG. 1. (a) Self-energy of the itinerant electrons at order $K^2(\mathbf{R})$. The hatched lines represent the local-moments spin-fluctuation propagator $\mathcal{D}(\omega_n, \mathbf{R}_1, \mathbf{R}_2)$. (b) The four-point function \mathcal{T} of the itinerant electrons: \mathcal{T}_C is the contribution of the Coulomb interactions in H_C and the X represents the static impurity potential.

As the right-hand side of Eq. (2.11) is independent of ω_n (apart from its sign), we have identified this contribution to Σ as the quasielastic spin-flip scattering rate $1/\tau_{qe}^s$.

Now we turn to the contribution of the sites in \mathcal{L}_d . Using the fact that $\mathcal{D}(\Omega_n, \mathbf{R})$ is an even function of Ω_n , Eq. (2.10) can be shown to be equivalent to

the fact that the maximum value of $\omega_{\mathbf{R}}$ was much smaller than the Fermi energy) means that techniques developed for the well-studied electron-phonon²⁰ and heavy-fermion systems¹⁴ can be used in the calculation. A first step is the calculation of the truncated density and spin vertex functions of the itinerant electrons: $\Gamma^d(\mathbf{k}, \epsilon_n; \mathbf{q}, \omega_n)$ and $\Gamma^s(\mathbf{k}, \epsilon_n; \mathbf{q}, \omega_n)$, where the itinerant-electron propagators carry the frequencies $\epsilon_n + \omega_n/2$ and $\epsilon_n - \omega_n/2$ and momenta $\mathbf{k} + \mathbf{q}/2$ and $\mathbf{k} - \mathbf{q}/2$. These vertex functions represent the density and spin components of the correlation functions:

$$\Gamma_{\alpha\beta}(\mathbf{k}, \varepsilon_n; \mathbf{q}, \omega_n) G(\mathbf{k} + \mathbf{q}/2, \varepsilon_n + \omega_n/2) G(\mathbf{k} - \mathbf{q}/2, \varepsilon_n - \omega_n/2) \\ = \sum_{\gamma\delta} \int_0^\beta d\tau \int_0^\beta d\tau' \langle T_\tau [\gamma_{\gamma\delta}(\mathbf{q}, 0) c_{\mathbf{k}+\mathbf{q}/2, \alpha}^\dagger(\tau' - \tau/2) c_{\mathbf{k}-\mathbf{q}/2, \beta}(\tau' + \tau/2)] \rangle e^{i\varepsilon_n \tau} e^{i\omega_n \tau'} , \quad (2.14)$$

where

$$\gamma_{\alpha\beta}(\mathbf{q}) = \sum_{\mathbf{k}} c_{\mathbf{k}+\mathbf{q}/2, \alpha}^\dagger c_{\mathbf{k}-\mathbf{q}/2, \beta} .$$

We will examine the values of these vertex functions in the limits $q \ll k_F$ and $\omega_n, \varepsilon_n \ll E_F$ and \mathbf{k} on the Fermi surface.

We begin by reviewing the Fermi-liquid properties of H_C . The nonquasiparticle part of the vertex functions is obtained in the limit $\mathbf{q} = 0$, and $\omega_n \rightarrow 0$. Ward identities¹⁰ following from spin and density conservation constrain these vertex functions as follows:

$$\Gamma_C^d(\mathbf{k}, \varepsilon_n; \mathbf{q} = 0, \omega_n \rightarrow 0) = \frac{1}{a_C} , \quad (2.15) \\ \Gamma_C^s(\mathbf{k}, \varepsilon_n; \mathbf{q} = 0, \omega_n \rightarrow 0) = \frac{1}{a_C} .$$

A subscript C has been added to the vertex functions to emphasize that they involve only the interactions in H_C . Inclusion of the quasiparticle pieces of the response functions involves introduction of the four-point function \mathcal{T} shown in Fig. 1(b). The contribution \mathcal{T}_C of H_C is represented as usual in the form

$$\mathcal{T}_{\alpha\beta\gamma\delta; C}(\mathbf{k}, \varepsilon_n; \mathbf{k}', \varepsilon'_n; \mathbf{q}, \omega_n) \\ = \frac{1}{2N_C a_C^2} \{ F_C^s(\cos^{-1}[\mathbf{k} \cdot \mathbf{k}' / (|\mathbf{k}| |\mathbf{k}'|)]) \delta_{\alpha\gamma} \delta_{\beta\delta} \\ + F_C^a(\cos^{-1}[\mathbf{k} \cdot \mathbf{k}' / (|\mathbf{k}| |\mathbf{k}'|)]) \sigma_{\alpha\gamma}^\mu \sigma_{\beta\delta}^\mu \} . \quad (2.16)$$

As is usual¹⁰ we will neglect the \mathbf{q} , ε_n , ε'_n , and ω_n dependence of the interaction parameters F_C^s and F_C^a and retain only their dependence upon the angle between \mathbf{k} and \mathbf{k}' . In the hydrodynamic limit $\omega_n \tau_e \ll 1$, $q k_F \tau_e \ll m_C$ and purely s -wave impurity scattering, the only quantities which enter the response functions are the angular averages of F_C^s and F_C^a over the Fermi surface. As we shall just be considering the hydrodynamic limit in this paper, we will henceforth only retain the angular averages F_{0C}^s and F_{0C}^a , of the parameters F_C^s and F_C^a .

The presence of the local moments and the impurity scattering lead to additional terms in the expression for \mathcal{T} . These are shown schematically in Fig. 1(b). Retaining only the terms which are consistent with our approximations for the self-energy we obtain

$$T \sum_{\varepsilon_n} \sum_{\mathbf{k}} G(\mathbf{k} + \mathbf{q}/2, \varepsilon_n + \omega_n/2) G(\mathbf{k} - \mathbf{q}/2, \varepsilon_n - \omega_n/2) f(\varepsilon_n) \\ = i\pi N_C a_C^2 T \sum_{\varepsilon_n} \int \frac{d\Omega_n}{4\pi} \frac{\Theta(\varepsilon_n + \omega_n/2) - \Theta(\varepsilon_n - \omega_n/2)}{i\omega_n Z - (k_F/m_C) \mathbf{q} \cdot \mathbf{n} + (i/\tau_e + i/\tau_{qe}^s) \text{sgn}(\omega_n)} f(\varepsilon_n) - f(\infty) N_C a_C^2 . \quad (2.20)$$

$$\mathcal{T}_{\alpha\beta\gamma\delta}(\varepsilon_n; \varepsilon'_n; \omega_n) = \mathcal{T}_{\alpha\beta\gamma\delta; C} \\ + \sum_{\mathbf{R}} K^2(\mathbf{R}) \mathcal{D}(\varepsilon_n - \varepsilon'_n, \mathbf{R}) \sigma_{\alpha\beta}^\mu \sigma_{\delta\gamma}^\mu \\ - \sum_{\mathbf{R}} K^2(\mathbf{R}) \mathcal{D}(\omega_n, \mathbf{R}) \sigma_{\alpha\gamma}^\mu \sigma_{\delta\beta}^\mu \\ + \frac{1}{2\pi N_C a_C^2} \delta_{\varepsilon_n, \varepsilon'_n} \delta_{\alpha\beta} \delta_{\delta\gamma} . \quad (2.17)$$

The right-hand side of this equation is independent of \mathbf{q} , \mathbf{k} , and \mathbf{k}' and the explicit dependence of \mathcal{T} upon these parameters has therefore been omitted. Instead of carrying explicitly the dependence of \mathcal{T} upon the spin indices, it is convenient at this early juncture to split \mathcal{T} into the components \mathcal{T}^d and \mathcal{T}^s , which will appear in the density and spin vertex functions, respectively. Using standard methods we find

$$\mathcal{T}^d(\varepsilon_n; \varepsilon'_n; \omega_n) = \frac{F_{0C}^3}{N_C a_C^2} + 3 \sum_{\mathbf{R}} K^2(\mathbf{R}) \mathcal{D}(\varepsilon_n - \varepsilon'_n, \mathbf{R}) \\ + \frac{1}{2\pi N_C a_C^2} \delta_{\varepsilon_n, \varepsilon'_n} , \quad (2.18) \\ \mathcal{T}^s(\varepsilon_n; \varepsilon'_n; \omega_n) = \frac{F_{0C}^a}{N_C a_C^2} - \sum_{\mathbf{R}} K^2(\mathbf{R}) \mathcal{D}(\varepsilon_n - \varepsilon'_n, \mathbf{R}) \\ - 2 \sum_{\mathbf{R}} K^2(\mathbf{R}) \mathcal{D}(\omega_n, \mathbf{R}) + \frac{1}{2\pi N_C a_C^2} \delta_{\varepsilon_n, \varepsilon'_n} .$$

We are now in a position to write down explicitly the integral equations satisfied by the vertex functions Γ^d and Γ^s including the all the interactions in the Hamiltonian H . The equation for the truncated density vertex function is

$$\Gamma^d(\varepsilon_n; \mathbf{q}, \omega_n) = \frac{1}{a_C} + T \sum_{\varepsilon'_n} \sum_{\mathbf{k}'} \Gamma^d(\varepsilon'_n; \mathbf{q}, \omega_n) \mathcal{T}^d(\varepsilon'_n; \varepsilon_n; \omega_n) \\ \times G(\mathbf{k}' + \mathbf{q}/2, \varepsilon'_n + \omega_n/2) \\ \times G(\mathbf{k}' - \mathbf{q}/2, \varepsilon'_n - \omega_n/2) , \quad (2.19)$$

where the Green's functions now include only the quasiparticle pieces. The equation for the spin vertex function is identical with the d 's replaced by s 's. This integral equation can be solved by generalizing the techniques developed by Leggett¹³ for the electron-phonon problem. The solution depends upon the following identity, whose validity is established in Ref. 13:

Here $f(\epsilon_n)$ is an arbitrary function of ϵ_n , which varies on a scale $\Lambda = \max(\omega_R)$, Λ satisfies $\Lambda \ll E_F$, and $f(\infty)$ represents $f(\epsilon_n \gg \Lambda)$. In deriving this result we have also used the fact that $Z(\omega_n \gg \Lambda) \searrow 1$. By repeated applications of the identity in Eq. (2.20) to Eq. (2.19) and by using the approximations made in the evaluation of the self-energy, it can be shown that the integral equation in Eq. (2.19) reduces to algebraic equations in the following quantities:

$$\Gamma_{\pm}^d = \Gamma^d(\epsilon_n \ll \Lambda; \mathbf{q}, \omega_n), \quad (\epsilon_n + \omega_n/2)(\epsilon_n - \omega_n/2) < 0 \quad (2.21a)$$

$$\Gamma_{\oplus}^d = \Gamma^d(\epsilon_n \ll \Lambda; \mathbf{q}, \omega_n), \quad (\epsilon_n + \omega_n/2)(\epsilon_n - \omega_n/2) > 0 \quad (2.21b)$$

$$\Gamma_{\infty}^d = \Gamma^d(\epsilon_n \gg \Lambda; \mathbf{q}, \omega_n). \quad (2.21c)$$

The left-hand sides of these equations are implicitly dependent upon \mathbf{q} and ω_n ; these dependences have not been made explicit to make the subsequent notation compact. Exactly similar representations are also made for the spin vertex functions.

Following the procedure above finally produces the following equations for the density vertex function:

$$\Gamma_{\pm}^d = \frac{1}{a_C} + \Gamma_{\pm}^d Q \operatorname{sgn}(\omega_n) \left(\frac{1}{\tau_e} + \frac{1}{\tau_{qe}^s} \right) + \Gamma_{\pm}^d Q \omega_n (F_{0C}^s + Z - 1) - \Gamma_{\infty}^d F_{0C}^s, \quad (2.22a)$$

$$\Gamma_{\oplus}^d = \frac{1}{a_C} + \Gamma_{\pm}^d Q \omega_n (F_{0C}^s + Z - 1) - \Gamma_{\infty}^d F_{0C}^s, \quad (2.22b)$$

$$\Gamma_{\infty}^d = \frac{1}{a_C} + \Gamma_{\pm}^d Q \omega_n F_{0C}^s - \Gamma_{\infty}^d F_{0C}^s, \quad (2.22c)$$

where

$$Q = \int \frac{d\Omega_n}{4\pi} \times \frac{1}{Z\omega_n + i(k_F/m_C)\mathbf{q} \cdot \mathbf{n} + \operatorname{sgn}(\omega_n)(1/\tau_e + 1/\tau_{qe}^s)}. \quad (2.23)$$

In the hydrodynamic limit Q reduces to

$$Q = \operatorname{sgn}(\omega_n)\tau(1 - Dq^2\tau - |\omega_n|\tau), \quad (2.24)$$

where D and τ were defined in the Introduction.

In a similar manner we obtain the equations for the spin vertex functions yield:

$$\Gamma_{\pm}^s = \frac{1}{a_C} + \Gamma_{\pm}^s Q \operatorname{sgn}(\omega_n) \left(\frac{1}{\tau_e} - \frac{1}{3\tau_{qe}^s} \right) + \Gamma_{\pm}^s Q \omega_n \left[\bar{F}^a - \frac{Z-1}{3} \right] - \Gamma_{\infty}^s \bar{F}^a, \quad (2.25a)$$

$$\Gamma_{\oplus}^s = \frac{1}{a_C} + \Gamma_{\pm}^s Q \omega_n \left[\bar{F}^a - \frac{Z-1}{3} \right] - \Gamma_{\infty}^s \bar{F}^a, \quad (2.25b)$$

$$\Gamma_{\infty}^s = \frac{1}{a_C} + \Gamma_{\pm}^s Q \omega_n \bar{F}^a - \Gamma_{\infty}^s \bar{F}^a, \quad (2.25c)$$

where

$$\bar{F}^a = F_{0C}^a - 2N_C a_C^2 \sum_{\mathbf{R}} K^2(\mathbf{R}) \mathcal{D}(\omega_n, \mathbf{R}). \quad (2.26)$$

The value of the Fermi-liquid constant \bar{F}^a used in the thermodynamic response functions in the Introduction is obtained by putting $\omega_n = 0$ in Eq. (2.26).

The Eqs. (2.22) and (2.25) can easily be solved and we obtain the following results for the density vertex functions,

$$\Gamma_{\pm}^d = \frac{1}{a_C \tau} \frac{1}{|\omega_n| + (1 + F_{0C}^s) D q^2}, \quad (2.27a)$$

$$\Gamma_{\oplus}^d = \frac{1}{a_C} \frac{Z|\omega_n| + D q^2}{|\omega_n| + (1 + F_{0C}^s) D q^2}, \quad (2.27b)$$

$$\Gamma_{\infty}^d = \frac{1}{a_C} \frac{|\omega_n| + D q^2}{|\omega_n| + (1 + F_{0C}^s) D q^2}, \quad (2.27c)$$

and for the spin vertex functions

$$\Gamma_{\pm}^s = \frac{1}{a_C \tau} \frac{1}{[D q^2 + 4/(3\tau_{qe}^s) + |\omega_n| 4(Z-1)/3](1 + \bar{F}^a) + |\omega_n|}, \quad (2.28a)$$

$$\Gamma_{\oplus}^s = \frac{1}{a_C} \frac{Z|\omega_n| + D q^2 + 4/(3\tau_{qe}^s)}{[D q^2 + 4/(3\tau_{qe}^s) + |\omega_n| 4(Z-1)/3](1 + \bar{F}^a) + |\omega_n|}, \quad (2.28b)$$

$$\Gamma_{\infty}^s = \frac{1}{a_C} \frac{|\omega_n| (4Z-1)/3 + D q^2 + 4/(3\tau_{qe}^s)}{[D q^2 + 4/(3\tau_{qe}^s) + |\omega_n| 4(Z-1)/3](1 + \bar{F}^a) + |\omega_n|}. \quad (2.28c)$$

Finally, we use the expressions for the vertex functions to calculate Π^d , the polarization function and χ^s , the spin-response function, of the itinerant electrons. We use the relationship

$$\chi^x(\mathbf{q}, \omega_n) = -T \sum_{\epsilon_n} \sum_{\mathbf{k}} \Gamma^x(\mathbf{q}, \omega_n) G(\mathbf{k} + \mathbf{q}/2, \epsilon_n + \omega_n/2) G(\mathbf{k} - \mathbf{q}/2, \epsilon_n - \omega_n/2), \quad (2.29)$$

where $x = (d, s)$. Using the identity (2.20) this equation reduces to

$$\chi^x = -N_C a_C (\Gamma_{\pm}^x Q \omega_n - \Gamma_{\infty}^x). \quad (2.30)$$

Evaluating Eq. (2.30) we obtain finally the following expressions for the density and spin-response functions of the itinerant electrons:

$$\begin{aligned}\Pi^d(q, \omega_n) &= N_C \frac{Dq^2}{Dq^2(1+F_{0C}^s) + |\omega_n|}, \\ \chi^s(q, \omega_n) &= N_C \frac{Dq^2 + 4/(3\tau_{qe}^s) + |\omega_n|4(Z-1)/3}{[Dq^2 + 4/(3\tau_{qe}^s) + |\omega_n|4(Z-1)/3](1+\bar{F}^a) + |\omega_n|}.\end{aligned}\quad (2.31)$$

Analytic continuation of these expressions to real frequencies leads to the expressions in Eq. (1.4) in the Introduction.

III. DISORDERED-ANDERSON-MODEL CALCULATION

In this section we perform a simple calculation on a disordered Anderson model¹⁷ to illustrate explicitly the general theory discussed in the previous section. The calculation also sheds light on the nature of the *total* transverse spin-correlation function (involving the sum of the itinerant-electron and local-moment spins) which is measured in an ESR experiment. In particular we will demonstrate how, when the g factors of the itinerant electrons and local moments are equal, the cutoff $1/(\tau_{qe}^s)$ can appear in the itinerant electron spin-correlation function but not in the total spin-correlation function. The local moments are represented by localized orbitals at the sites \mathbf{R}_i , with the electron creation operators at these sites being $c_{d,\alpha}^\dagger$. The subscript d simply distinguishes these sites from the itinerant electrons and does not refer to an orbital with d -like symmetry. The Hamiltonian we shall consider is

$$\begin{aligned}H_A &= \sum_{\mathbf{k}, \alpha} \varepsilon_{\mathbf{k}} c_{\mathbf{k}, \alpha}^\dagger c_{\mathbf{k}, \alpha} + \sum_{\mathbf{k}, \alpha} \sum_i V [c_{\mathbf{k}, \alpha}^\dagger c_{d, \alpha}(i) + \text{H.c.}] e^{i\mathbf{k} \cdot \mathbf{R}_i} + \sum_i \varepsilon_d [n_{d\uparrow}(i) + n_{d\downarrow}(i)] \\ &+ \sum_i U n_{d\uparrow}(i) n_{d\downarrow}(i) + \frac{1}{2} h \sum_{\mathbf{k}} (c_{\mathbf{k}\uparrow}^\dagger c_{\mathbf{k}\uparrow} - c_{\mathbf{k}\downarrow}^\dagger c_{\mathbf{k}\downarrow}) + \frac{1}{2} h \sum_i [n_{d\uparrow}(i) - n_{d\downarrow}(i)] + H_{\text{dis}},\end{aligned}\quad (3.1)$$

where $n_{d\alpha} = c_{d\alpha}^\dagger c_{d\alpha}$, U is repulsion between two opposite-spin electrons on the same site, h is a magnetic field pointing in the z direction (the g factors of the itinerant electrons and local moments are equal and have been absorbed into the definition of h), and H_{dis} , which was displayed explicitly in Eq. (2.6), is the random static potential scattering the itinerant electrons. The coupling between the conduction electrons and the local moments is represented by the hybridization parameter V . In this respect H_A differs from the Hamiltonian considered in the previous section, which had an exchange coupling between the local moments and itinerant electrons. The advantage of the hybridization coupling is that it simplifies the integral equations for the vertex functions into a separable form and also allows for a straightforward calculation of the local-moment spin-correlation functions. In addition, the well-known Schrieffer-Wolff²¹ transformation shows the two types of coupling to be equivalent in the large- U limit. To obtain a finite spin-relaxation rate of the conduction electrons at a low order in the perturbation theory it will be necessary to work in the broken-symmetry phase of Anderson's Hartree-Fock theory.¹⁷ The local moments will be assumed to be polarized in the z direction with a magnetization m . They will appear to the itinerant electrons simply as quasistatic impurity potentials which scatter up and down electrons with different strengths. However, the transverse fluctuations of the local moments will be shown to be of just the right magnitude to lead to an infinitely sharp ESR line. A drawback of the present approach is that the itinerant-electron correlation functions are not explicitly rotationally invariant even in the zero-field limit; the comparison with the results of Sec. II must therefore be performed with some care. We also note here that different aspects

of a similar model have been studied earlier by Caroli, Caroli, and Fredkin.²²

The lowest-order terms for the self-energy of the conduction electrons are shown in Fig. 2(a). The single lines represent the conduction electrons, the double lines the local moments, and the solid circles represent the interaction V . The conduction-electron Green's function has the form

$$G_\alpha^c(\mathbf{k}, \omega_n) = \frac{1}{i\omega_n - \varepsilon_{\mathbf{k}} - \alpha h/2 - cV^2 G_\alpha^d(\omega_n) + i \text{sgn}(\omega_n)/2\tau_e},\quad (3.2)$$

where $\alpha = \pm 1$ is the spin, c is the concentration of local moments, and G_α^d is the local-moment Green's function. The positions of the local moments have been averaged over all space. We will consider, for simplicity, properties of the local moments only in the particle-hole symmetric case with $\varepsilon_d = -U/2$. Under these circumstances, the mean occupation numbers of the local-moment sites have the form

$$n_{d\uparrow} = \frac{1}{2} + \frac{m}{2}, \quad n_{d\downarrow} = \frac{1}{2} - \frac{m}{2},\quad (3.3)$$

where m is the local-moment magnetization. The local-moment Green's function G_α^d has the value

$$G_\alpha^d(\omega_n) = \frac{1}{i\omega_n - \alpha(h/2 - Um/2) + i\Delta \text{sgn}(\omega_n)},\quad (3.4)$$

where $\Delta = \pi V^2/N$ is the width of the d resonance, N is the density of states of the conduction electrons, and m is given by the self-consistency condition

$$m = \int_{-\infty}^{\infty} \frac{d\omega}{\pi} f(\omega) \left[\frac{\Delta}{(\omega - h/2 + Um/2)^2 + \Delta^2} - \frac{\Delta}{(\omega + h/2 - Um/2)^2 + \Delta^2} \right], \quad (3.5)$$

where $f(\omega)$ is the Fermi function.

We now proceed to a calculation of the response functions of the system in an approximation consistent with the Green's functions displayed above. We will consider the transverse spin-correlation functions, as they are the ones measured in an ESR experiment. The calculations for the density and longitudinal spin-response functions can be carried out in a similar manner. Unless explicitly stated otherwise, all the four-point, vertex, and response functions introduced below will refer to their transverse spin components. We begin by considering the local-moment four-point function T_0^{dd} ; the equation satisfied by this four point function is shown in Fig. 2(b). The subscript 0 emphasizes that this four-point function involves no intermediate itinerant-electron electrons. The diagrams in Fig. 2(b) leads to the expression

$$T_0^{dd}(\omega_n) = - \frac{U}{1 + UT \sum_{\epsilon_n} G_{\uparrow}^d(\epsilon_n + \omega_n/2) G_{\downarrow}^d(\epsilon_n - \omega_n/2)}. \quad (3.6)$$

In the following calculation we will consider only the case $\omega_n > 0$. The frequency summation in the denominator of Eq. (3.6) can be carried out as follows:

$$T \sum_{\epsilon_n} G_{\uparrow}^d(\epsilon_n + \omega_n/2) G_{\downarrow}^d(\epsilon_n - \omega_n/2) = \frac{1}{-i\omega_n + h - Um} \left[+2i\Delta T \sum_{-\omega_n/2 < \epsilon_n < \omega_n/2} G_{\uparrow}^d(\epsilon_n + \omega_n/2) G_{\downarrow}^d(\epsilon_n - \omega_n/2) \right] \\ \approx \frac{1}{-i\omega_n + h - Um} \left[m + \frac{i\Delta P \omega_n}{\pi} \right], \quad (3.7)$$

where we have introduced the quantity

$$P \equiv - \frac{1}{(Um/2 + i\Delta)^2}. \quad (3.8)$$

The summation in over ϵ_n between $-\omega_n/2$ and $\omega_n/2$ has been carried out in the limit $\omega_n, h \ll \Delta, Um$ corresponding to a low external frequency and magnetic field. We will also need below the local-moment vertex function Γ_0^{dd} , which is defined by the equation

$$\Gamma_0^{dd}(\omega_n) = 1 + T \sum_{\epsilon_n} G_{\uparrow}^d(\epsilon_n + \omega_n/2) G_{\downarrow}^d(\epsilon_n - \omega_n/2) T_0^{dd}(\omega_n), \quad (3.9)$$

and the subscript 0 again emphasizes that intermediate conduction-electron interactions have not yet been included. The frequency summation can be carried out as in Eq. (3.7) and yields

$$\Gamma_0^{dd}(\omega_n) = \frac{-i\omega_n + h - Um}{-i\omega_n + h + i\Delta P U \omega_n / \pi}. \quad (3.10)$$

Using the four-point function T_0^{dd} we show in Fig. 3 an expression for the conduction-electron vertex function Γ^{cc} . This is the *full* vertex function, involving all possible itinerant-electron and local-moment interactions, and therefore does not have a subscript 0. The equation for Γ^{cc} can be solved very simply after making the following approximations: (i) replace all summations over a frequency ϵ_n between $-\omega_n/2$ and $\omega_n/2$ by a factor of $\omega_n/(2\pi T)$; and (ii) replace all $G_{\uparrow}^d G_{\downarrow}^d$ factors in the argument of this summation by P . These same approximations were made in the evaluation of Eq.

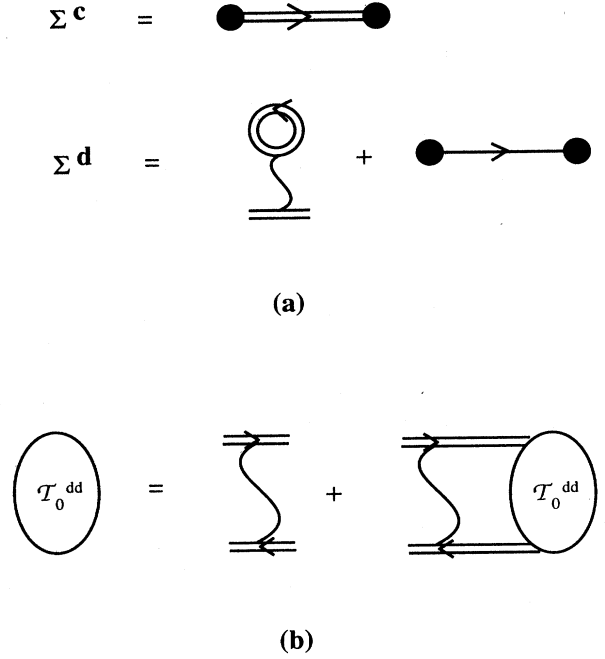


FIG. 2. (a) Self-energy of the conduction electrons (Σ^c) and the local moments (Σ^d). The single lines represent the conduction electrons, the double lines represent the local moments, the solid circle represents the hybridization parameter V and the wavy line is the Hubbard interaction U . (b) The four-point function of the local moments T_0^{dd} .

(3.7). This procedure yields

$$\Gamma^{cc}(\mathbf{q}, \omega_n) = \frac{1}{1 - 2cV^2\Delta P Q - Q/\tau_e - cV^2\Delta P^2 Q T_0^{dd}(\omega_n)\omega_n/\pi}, \quad (3.11)$$

where Q is the analog of the Q introduced in Eq. (2.23) and is given by the expression

$$\begin{aligned} Q(\varepsilon_n; \mathbf{q}, \omega_n) &= \frac{1}{2\pi N} \sum_{\mathbf{k}} G_{\uparrow}^c(\mathbf{k} + \mathbf{q}/2, \varepsilon_n + \omega_n/2) G_{\downarrow}^c(\mathbf{k} - \mathbf{q}/2, \varepsilon_n - \omega_n/2) \\ &= \int \frac{d\Omega_n}{4\pi} \frac{1}{\omega_n + ih + i(k_F/m)\mathbf{q} \cdot \mathbf{n} + 1/\tau_e + icV^2[G_{\uparrow}^d(\varepsilon_n + \omega_n/2) - G_{\downarrow}^d(\varepsilon_n - \omega_n/2)]}. \end{aligned} \quad (3.12)$$

In the hydrodynamic limit $|\omega_n| \tau_e, k_F q \tau_e / m \ll 1$, and, making the approximations (i) and (ii) enumerated above, we find

$$Q^{-1}(\mathbf{q}, \omega_n) \approx \frac{1}{\tau_e} + 2cV^2\Delta P + (\omega_n + ih)(1 + cV^2P) - icV^2P U m + D q^2, \quad (3.13)$$

where D is the diffusion constant given by $D = k_F^2 \tau / (3m^2)$ with

$$\frac{1}{\tau} \approx \frac{1}{\tau_e} + 2cV^2\Delta P. \quad (3.14)$$

Finally, we use the vertex function Γ^{cc} to evaluate the conduction-electron transverse spin correlation function χ^{cc} :

$$\begin{aligned} \chi^{cc}(\mathbf{q}, \omega_n) &= -T \sum_{\varepsilon_n} \sum_{\mathbf{k}} G^c(\mathbf{k} + \mathbf{q}/2, \varepsilon_n + \omega_n/2) G^c(\mathbf{k} - \mathbf{q}/2, \varepsilon_n - \omega_n/2) \Gamma^{cc}(\mathbf{q}, \omega_n) \\ &= N \left[1 - \frac{\omega_n}{Q^{-1} - 2cV^2\Delta P - 1/\tau_e - cV^2\Delta P^2 T_0^{dd}(\omega_n)\omega_n/\pi} \right]. \end{aligned} \quad (3.15)$$

Using the expression for Q^{-1} in Eq. (3.13) we obtain, in zero external magnetic field $h=0$,

$$\begin{aligned} \chi^{cc}(\mathbf{q}, \omega_n; h=0) &= N \frac{Dq^2 + 4/(3\tau_{qe}^s) + |\omega_n|4(Z-1)/3}{[Dq^2 + 4/(3\tau_{qe}^s)|\omega_n|4(Z-1)/3] + |\omega_n|}, \end{aligned} \quad (3.16)$$

where we have defined

$$\frac{4}{3\tau_{qe}^s} = icV^2 \frac{Um}{(Um/2 + i\Delta)^2 + \Delta U/\pi} \quad (3.17)$$

and

$$Z = 1 - \frac{3cV^2}{4} \frac{1}{(Um/2 + i\Delta)^2}. \quad (3.18)$$

Comparing this to Eq. (2.31) we find that Eq. (3.16) has the form demanded by Fermi-liquid theory with $\tilde{F}^a=0$. The lack of terms in the local-moments spin-fluctuation propagator of H_A which survive the limit $\varepsilon_n \rightarrow \infty$, is responsible for the vanishing of \tilde{F}^a . Unlike Sec. II, the values of the parameters D , Z , and τ_{qe}^s are now complex. This is a consequence of the broken spin symmetry of the local moments. The polarization of the local moments in the z direction produces an internal field, about which the spins of the itinerant electrons precess. The imaginary parts of Z , D , and τ_{qe}^s are a direct consequence of this precession. These parameters should, however, be real in the longitudinal spin-correlation (χ_z^{cc}) and the density-correlation (Π^{cc}) functions because the internal field is polarized in the z direction. We find

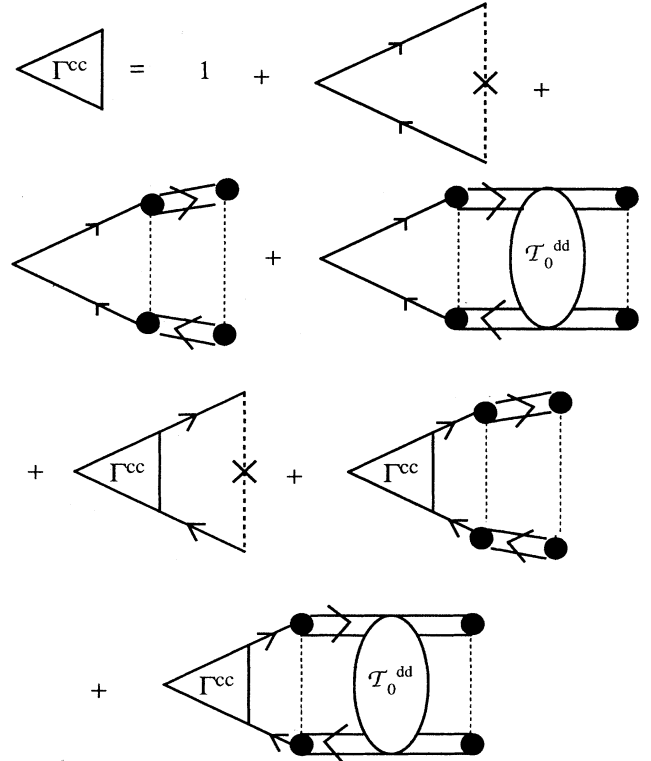


FIG. 3. The integral equation for the conduction-electron vertex function Γ^{cc} . The dashed lines connecting the solid circles signify that the hybridization occurs at the same local-moment site.

$$\chi_z^{cc}(\mathbf{q}, \omega_n; h=0) = N \frac{Dq^2 + |\omega_n| 4(\tilde{Z}_a - 1)/3}{[Dq^2 + |\omega_n| 4(\tilde{Z}_a - 1)/3] + |\omega_n|}, \quad (3.19)$$

where

$$\tilde{Z}_a = 1 + \frac{3cV^2}{4} \frac{1}{(Um/2)^2 + \Delta^2 + a\Delta U/\pi}, \quad (3.20)$$

and $a = -1$. The expression for Π^{cc} is identical but has $a = 1$. The value of τ in the expression for D is now given by

$$\frac{1}{\tau} = \frac{1}{\tau_e} + \frac{2cV^2\Delta}{(Um/2)^2 + \Delta^2}. \quad (3.21)$$

We note (i) \tilde{Z}_a and τ are real; (ii) the relaxation rate $1/\tau_{qe}^s$ is zero for the longitudinal spin—this feature will not occur in a calculation which includes terms which are higher order in the coupling V ; (iii) there is a frequency renormalization factor \tilde{Z}_a in the expression of Π^{cc} —this is because, unlike the model of Sec. II, the number of conduction electrons is not conserved by H_A .

The remaining part of this section pushes the model calculation beyond what could have been anticipated by

general Fermi-liquid considerations. We begin by calculating the local-moment transverse spin-correlation function

$$\chi_0^{dd}(\omega_n) = -T \sum_{\epsilon_n} G_{\uparrow}^d(\epsilon_n + \omega_n/2) G_{\downarrow}^d(\epsilon_n - \omega_n/2) \Gamma_0^{dd}(\omega_n), \quad (3.22)$$

where the subscript 0 has been introduced to emphasize the absence of intermediate conduction-electron states. Evaluating the frequency summation we find

$$\chi_0^{dd}(\omega_n) = -\frac{m + i\Delta P \omega_n / \pi}{-i\omega_n + h + i\Delta P U \omega_n / \pi}. \quad (3.23)$$

We are now in a position to calculate the total electron transverse spin-correlation function χ_t including the contributions of the cross-correlations between the itinerant electrons and the local momenta. The expression for χ_t in terms of all the quantities introduced so far is shown in Fig. 4. We have also introduced a conduction-electron four-point function \mathcal{T}^{cc} which is related to the vertex function Γ^{cc} by the conduction-electron analog of Eq. (3.9). With the usual approximations, the diagrams in Fig. 4 lead to the equation

$$\chi_t(\mathbf{q}, \omega_n) = N + c\chi_0^{dd}(\omega_n) - (1 + cV^2 P \Gamma_0^{dd})^2 \frac{N\omega_n}{Q^{-1} - 2cV^2 \Delta P - 1/\tau_e - cV^2 \Delta P^2 \mathcal{T}_0^{dd}(\omega_n) \omega_n / \pi}. \quad (3.24)$$

Although complicated in appearance, this expression for χ_t can be reduced to a very simple form in the limit $\mathbf{q} = \mathbf{0}$. Using the expressions for χ_0^{dd} , Γ_0^{dd} , and \mathcal{T}_0^{dd} in Eqs. (3.23), (3.10), (3.6), (3.7), and (3.8), we find after analytic continuation to the real frequency axis

$$\chi_t(\mathbf{q} = \mathbf{0}, \omega_n) = \frac{cm}{\omega - h} + \frac{-Nh}{\omega - h}. \quad (3.25)$$

This equation has a simple pole at $\omega = h$ corresponding to an infinitely sharp ESR line. The susceptibility χ is seen to be a simple sum of itinerant-electron and local-moment contributions. For $\omega = 0$ the local-moment contribution is $-cm/h$. This is exactly the form required in a system with broken spin symmetry and the divergence in the susceptibility as $h \rightarrow 0$ is a signal of the Goldstone fluctuations. Finally, this expression for χ_t is consistent with the ansatz discussed in Eq. (1.7) in the Introduction.

IV. APPLICATION TO EXPERIMENTS

The new quantity introduced in this paper is the spin-flip quasielastic scattering rate $1/\tau_{qe}^s$; a direct consequence of this scattering which is potentially measurable in experiments is the temperature dependence of the conductivity induced by the relationship

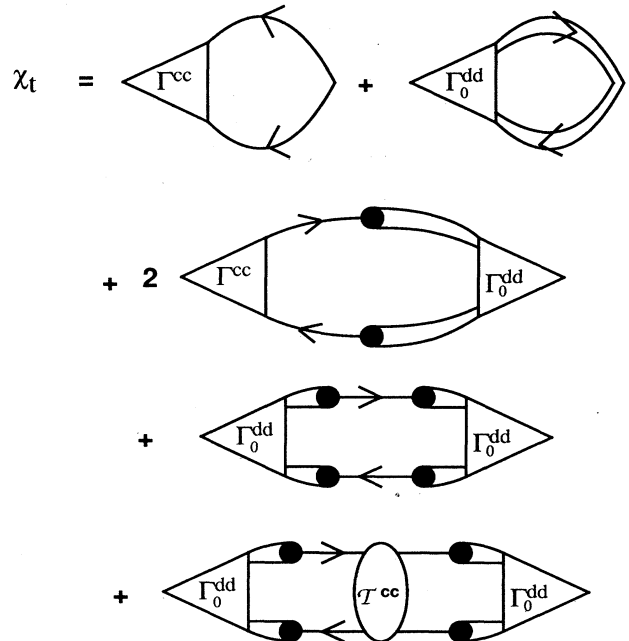


FIG. 4. Expression for the total transverse spin susceptibility χ_t in terms of the vertex functions introduced earlier.

$$\sigma = e^2 N_C \frac{k_F^2}{3m_C^2} \tau \quad (4.1)$$

and Eq. (1.5). To test this relationship we begin by establishing a simple correlation between the temperature dependence of τ_{qe}^s and that of the local-moment static spin susceptibility. Using the constraint on the equal-time correlation function $\langle S_\mu S_\nu \rangle = \frac{1}{4} \delta_{\mu\nu}$ at *each* local moment site \mathbf{R} , we obtain

$$T \sum_{\Omega_n} \mathcal{D}(\Omega_n, \mathbf{R}) = \frac{1}{4}. \quad (4.2)$$

Equation (2.11) therefore simplifies to

$$\frac{1}{\tau_{qe}^s} = \frac{3\pi N_C a_C^2 \overline{K^2(\mathbf{R})} n_f}{8}, \quad (4.3)$$

where $\overline{K^2(\mathbf{R})}$ is the mean square average of the couplings $K(\mathbf{R})$ and n_f is the number of free local moments, i.e., local moments with $\omega_{\mathbf{R}} < T$. The calculation of Ref. 12 showed that static spin susceptibility of the local moments (χ^L) was nearly equal to $n_f/(2T)$. We therefore obtain the simple expression

$$\frac{\Delta\sigma(T)}{\sigma} \approx \tau \frac{-3\pi N_C a_C^2 \overline{K^2(\mathbf{R})} [2T\chi^L(T)]}{8} \quad (4.4)$$

for the change in the conductivity $[\Delta\sigma(T)]$ induced by the interaction with the low-lying-spin local spin fluctuations. We have assumed here that $\tau \ll \tau_{qe}^s$.

Experimental testing of the above relationship is complicated by the \sqrt{T} temperature dependence of the conductivity induced by localization effects contained in the Hamiltonian $H_C + H_{\text{dis}}$.²³ We also know that the relationship cannot hold very close to the MIT because the conductivity *decreases* to 0 with falling temperatures at $n = n_c$. However, there is a regime of doping densities in Si:P ($1.05n_c \leq n \leq 1.5n_c$) where the Fermi-liquid theory of this paper is expected to be valid and the conductivity does increase with falling temperatures. If we now make the drastic oversimplifications of ignoring the localization effects and assuming that the total static spin susceptibility χ_t is dominated by χ^L , we obtain the simple relationship

$$\sigma(T) = \sigma_0 - cT\chi_t(T), \quad (4.5)$$

where $\sigma_0 = \sigma(T=0)$ and c is a temperature-independent constant whose value follows simply from Eq. (4.4). In Fig. 5 we have plotted $\sigma(T)$ versus T along with the best one-parameter fit to Eq. (4.5) for two different samples of Si:P. The fit is reasonable indicating that the temperature dependence of conductivity can be consistently interpreted as arising from slow local spin fluctuations. The values of the parameters σ_0 and c obtained from the fit are listed in Table I. The slightly larger value of c for the denser sample can be due to the increases in either the value of N_C or the value of $\overline{K^2(\mathbf{R})}$ [$\overline{K^2(\mathbf{R})}$ is larger because exchange constants are larger when the impurity sites are closer to each other]. The fit yields an estimate of $\tau_{qe}^s \approx 8\tau_e \approx (kT)^{-1}$ at 10 K. Taking the local-moment

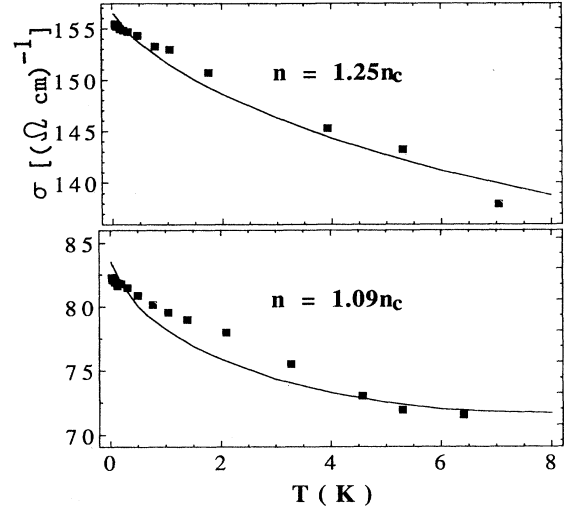


FIG. 5. The conductivity of two samples of Si:P as a function of T (solid lines). The squares represent the best fit to Eq. (4.5) using the measured susceptibility. (Unpublished data of M. A. Paalanen.)

picture literally and using values of n_f from Ref. 1 we obtain an estimate to $[\overline{K^2(\mathbf{R})}]^{1/2}$ of 5–10 K which is rather large: a full calculation of the formation of local moments is therefore necessary to understand the strength of the coupling between the itinerant quasiparticles and local spin fluctuations.

We emphasize again however that the neglect of the \sqrt{T} corrections is not justifiable and all Fig. 5 indicates is that the spin-flip quasielastic scattering yields a temperature dependence to the conductivity which is consistent with experiments, and should be considered on an equal footing with \sqrt{T} localization corrections in a more complete analysis. To really settle the issue of the relative importance of the spin-flip quasielastic scattering and the localization corrections it is important to perform experiments which have a different dependence upon the two quantities. A probe which will provide additional constraints is the magnetic field dependence of the conductivity. At zero temperature the magnetic field will polarize spins which were weakly locked into singlets and lead to increased scattering: the local moments therefore induce a positive magnetoresistance. The localization corrections of noninteracting electrons always have a negative magnetoresistance while those of interacting electrons can have either sign.

TABLE I. Values of the parameters σ_0 and c of Eq. (4.5) obtained from the experimental fits in Fig. 5.

n/n_c	σ_0 [(Ω cm) $^{-1}$]	c [10^8 (Ω cm) $^{-1}$ (emu K/cm 3) $^{-1}$]
1.09	83.0	0.21
1.25	155.9	0.28

V. CONCLUSIONS

This paper has presented a description of the Fermi-liquid properties of a new phenomenological Hamiltonian H designed to understand the finite-temperature properties of the metallic state near the MIT. The model consists of a fluid of itinerant electrons interacting with a dilute concentration of local moments placed randomly in space. The presence of the local moments leads to a temperature-dependent frequency renormalization factor $Z(T)$ and a temperature-dependent spin-flip quasielastic scattering rate $1/\tau_{qe}^s(T)$ in the itinerant-electron Green's functions. The factor $Z(T)$ does not affect the values of the compressibility, conductivity, or spin susceptibility. The itinerant-electron spin susceptibility is, however, enhanced by a temperature-independent decrease in the value of the Fermi-liquid parameter F_0^a due to the presence of the local moments. The presence of an interaction H_{int} between the itinerant electrons and the local moments therefore leads to an innocuous temperature-independent renormalization of the *thermodynamic* properties and justifies the neglect of H_{int} in Ref. 1. The spin-flip quasielastic scattering has two important consequences.

(i) It leads to a temperature dependence in the conductivity even with the Boltzmann approximation (temperature dependence from localization contributions only appears in terms which are higher order in disorder). The predictions of the theory provide a reasonable fit to experimental observations; the fit leads to a value of $1/\tau_{qe}^s \approx 10$ K at 10 K in Si:P.

(ii) The rate $1/\tau_{qe}^s$ acts as cutoff in the singlet and triplet particle-particle and triplet particle-hole ladders of the itinerant electrons. It will therefore have important consequences for any attempt to use the scaling theories of the MIT upon the itinerant electrons.

This paper also addressed the properties of the *total* electron spin susceptibility involving the itinerant electron and local-moment contributions and their cross correlations. This was done by examining a disordered Anderson model at the self-consistent one-loop level. In a finite magnetic field h and assuming that the g factors of

the local moments and itinerant electrons are equal, the spectral weight of the total transverse spin susceptibility was found to be a δ function at $\omega=h$. Thus the rate $1/\tau_{qe}^s$ does not act as a cutoff for the spin total susceptibility, and the ESR linewidth will arise solely from couplings to nuclear spins and the lattice. As noted in Ref. 9 the dominant contribution to the linewidth at low temperatures comes from the relaxation of the local moments by their hyperfine interaction A with the phosphorus nuclear spins.

Although not complete, our analysis should serve as a useful starting point for more sophisticated theories of the MIT. An important question which has not been addressed in this paper is the mechanism of the formation of electron local moments from a disordered Fermi fluid. Anderson solved the problem of local-moment formation on an impurity site with a tightly bound d orbital and a large Hubbard U .¹⁷ The strong interactions on the impurity site clearly distinguished it from other conduction-electron sites and lead to moment formation on the impurity site alone. In the present situation, the microscopic Hamiltonian can be approximated by a Hubbard model with random hopping matrix elements but with an equally strong U parameter on every site. The mechanism by which local moments form preferentially on some sites has not been addressed in this paper and is a problem which is currently being investigated.

Note added in proof. The question raised above has been addressed in a recent work.²⁴ This paper develops a criterion for the formation of local moments in a disordered Hubbard model.

ACKNOWLEDGMENTS

I would like to thank R. N. Bhatt and A. E. Ruckenstein for useful discussions and M. A. Paalanen for valuable comments and permission to present the data in Fig. 5. I am grateful to the IBM Thomas J. Watson Research Center (Yorktown Heights, NY) for hospitality while this work was being performed. This research was supported in part by the National Science Foundation.

¹M. A. Paalanen, J. Graebner, R. N. Bhatt, and S. Sachdev, Phys. Rev. Lett. **61**, 597 (1988).

²R. F. Milligan, T. F. Rosenbaum, R. N. Bhatt, and G. A. Thomas, in *Electron-Electron Interactions in Disordered Systems*, edited by A. L. Efros and M. Pollak (North-Holland, Amsterdam, 1985); P. A. Lee and T. V. Ramakrishnan, Rev. Mod. Phys. **57**, 287 (1985).

³A. M. Finkelstein, Zh. Eksp. Teor. Fiz. **84**, 166 (1983) [Sov. Phys.—JETP **57**, 97 (1983)]; Z. Phys. B **56**, 189 (1984); C. Castellani, C. DiCastro, P. A. Lee, and M. Ma, Phys. Rev. B **30**, 527 (1984).

⁴C. Castellani, B. G. Kotliar, and P. A. Lee, Phys. Rev. Lett. **56**, 1179 (1986).

⁵S. Sachdev, R. N. Bhatt, and M. A. Paalanen, J. Appl. Phys. **63**, 4285 (1988).

⁶R. N. Bhatt, M. A. Paalanen, and S. Sachdev, in Proceedings of

the International Conference on Magnetism, Paris, 1988 (unpublished).

⁷M. A. Paalanen, A. E. Ruckenstein, and G. A. Thomas, Phys. Rev. Lett. **54**, 1295 (1985); Z. Z. Gan and P. A. Lee, Phys. Rev. B **33**, 3595 (1986).

⁸J. D. Quirt and J. R. Marko, Phys. Rev. Lett. **26**, 318 (1971); H. Ue and S. Maekawa, Phys. Rev. B **3**, 4232 (1971).

⁹H. Alloul and P. Dellouve, Phys. Rev. Lett. **59**, 578 (1987).

¹⁰P. Nozières, *Theory of Interacting Fermi Systems* (Benjamin, New York, 1964).

¹¹O. Betbeder-Matibet and P. Nozières, Ann. Phys. (N.Y.) **37**, 17 (1966).

¹²R. N. Bhatt and P. A. Lee, Phys. Rev. Lett. **48**, 344 (1982).

¹³A. J. Leggett, Ann. Phys. (N.Y.) **46**, 76 (1968).

¹⁴C. M. Varma, Phys. Rev. Lett. **55**, 2723 (1985).

¹⁵K. Miyake, S. Schmitt-Rink, and C. M. Varma, Phys. Rev. B

- 34, 6554 (1986).
- ¹⁶H. Hasegawa, *Prog. Theor. Phys. (Kyoto)* **21**, 483 (1959).
- ¹⁷P. W. Anderson, *Phys. Rev.* **124**, 41 (1961).
- ¹⁸M. A. Paalanen, S. Sachdev, R. N. Bhatt, and A. E. Ruckenstein, *Phys. Rev. Lett.* **57**, 2061 (1986).
- ¹⁹S. Sachdev, *Phys. Rev. B* **34**, 6049 (1986); **35**, 7558 (1987).
- ²⁰D. J. Scalapino, in *Superconductivity*, edited by D. Parks (Dekker, New York, 1969), Vol. 1.
- ²¹J. R. Schrieffer and P. A. Wolff, *Phys. Rev.* **149**, 491 (1966).
- ²²B. Caroli, C. Caroli, and D. R. Fredkin, *Phys. Rev.* **178**, 599 (1969).
- ²³T. F. Rosenbaum, K. Andres, G. A. Thomas, and P. A. Lee, *Phys. Rev. Lett.* **46**, 568 (1981).
- ²⁴M. M. Lovanovic, S. Sachdev, and R. N. Bhatt (unpublished).